

Geometric properties of particle trajectories in turbulent flows

A. Scagliarini^{a*}*Department of Physics, University of Rome “Tor Vergata”,
Via della Ricerca Scientifica 1, 00133 Rome, Italy
(Received 00 Month 200x; final version received 00 Month 200x)*

We study the statistics of curvature and torsion of Lagrangian trajectories from direct numerical simulations of homogeneous and isotropic turbulence (at $Re_\lambda \approx 280$) in order to extract informations on the geometry of small scale coherent structures in turbulent flows. We find that, as previously observed by Braun *et al* [14] and by Xu *et al* [23], the high curvature statistics is dominated by large scale flow reversals where the velocity magnitude assumes very low values. In order to focus on small-scales signatures, we introduce a *cutoff* on the velocity amplitude and we study the probability distribution of time-filtered curvature conditioned only on those events when the local velocity is not that small. In this way we are able to select small-scales turbulent features, connected to vortex filaments. We show that the conditional probability density of time-filtered curvature is well reproduced by a multifractal formalism. Finally, by studying the joint statistics of curvature and torsion we find further evidences that intense and persistent events are dominated by helical type trajectories.

Keywords: Lagrangian turbulence; Chaotic advection; Differential geometry; Multifractals.

1. Introduction

The transport of particles in turbulent flows is an ubiquitous phenomenon relevant in very different physical contexts as cloud formation, pollutant dispersion, formation of “planetesimals” and turbulent mixing in chemical reactions [1–4]. To describe it, the optimal framework results to be the Lagrangian one, where flow properties are studied following the trajectories of individual fluid elements. Thus, understanding the Lagrangian statistics of particles advected by a turbulent velocity field $\mathbf{u}(\mathbf{x}, t)$ is a fundamental issue for both its theoretical implications (as, for instance, the development of stochastic models for dispersion and mixing) and for applications [1, 5, 7]. Lagrangian description is also more suitable than the Eulerian one to reveal the geometry and the statistical “weight” of coherent structures in turbulent flows. We cite here, for example, the preferential concentration of heavy/light particles inside hyperbolic/elliptic regions [18–20], the strong acceleration bursts experienced by tracers when following streamlines around vortex filaments [17] or the regularising effects of inertia in the transition from viscous scales to inertial range scales in the behaviour of Lagrangian Structure Functions [19]. Studies of Lagrangian turbulence mainly involve the analysis of the statistics of velocity (or vorticity) and acceleration [2, 6, 8–10, 17] (for an updated recent review see Toschi & Bodenschatz [11]). As suggested by Braun *et al.* [14], the trajectory of a Lagrangian particle $\mathbf{x} = \mathbf{x}(t)$ can be also seen as a set of parametric equations representing a spatial curve in 3D. As such it can be described by means of tools borrowed from differential geometry: in particular, it is well known that

*Corresponding author. Email: andrea.scagliarini@roma2.infn.it

a curve is uniquely determined by the knowledge at every point (or equivalently, in our “time-like” parameterization, at every instant of time) of two fundamental geometric parameters: the curvature κ and the torsion ϑ . They are related to the velocity (\mathbf{u}) and the acceleration (\mathbf{a}) of the particle by:

$$\kappa(t) = \frac{|\mathbf{u} \wedge \mathbf{a}|}{u^3} = \frac{a_{\perp}}{u^2} \quad (1)$$

(where a_{\perp} is the magnitude of the normal, or centripetal, acceleration) and

$$\vartheta(t) = \frac{\mathbf{u} \cdot (\mathbf{a} \wedge \dot{\mathbf{a}})}{\kappa^2 u^6}. \quad (2)$$

The torsion, unlike the curvature, has got a sign, which is related to the local helicity [12, 13]. Since we are not dealing with helical flows (that is we have a symmetric distribution of regions with positive and negative helicity, hence the same is for torsion), from now on we will refer to torsion discussing its absolute value $\theta = |\vartheta|$. Dimensionally κ and θ are an inverse length, so we may expect that they assume very high values in correspondence of the small scale structures we are interested in, namely the vortex filaments. It has been shown [6, 16, 17, 19] that such filaments are of great relevance in the Lagrangian statistics of turbulent velocity and acceleration for both tracers and inertial particles (playing in the latter case a crucial role in the mechanism responsible for the strong inhomogeneous particle spatial distribution). The aim of this work is twofold. First, we will further characterize the geometry of these coherent structures by studying the statistics of extreme values of curvature and torsion from Direct Numerical Simulations, extending the previous analysis made in [14] to higher Reynolds numbers and supporting the numerical results with a phenomenological description in terms of the multifractal theory. Second, thanks to the high Lagrangian statistics, we will also present joint statistics of torsion and curvature, highlighting the intimate geometrical structure of small scales intense vorticity in turbulent flows.

The paper is organized as follows. In section 2 we discuss the statistics of instantaneous and time-averaged (and conditioned on velocity values) curvature, in the latter case deriving some analytical results in the framework of the multifractal formalism; in section 3 we analyze the joint statistics of curvature and torsion in order to stress its connection with the topology of small-scale coherent structures. Conclusions and perspectives are left to the last section.

2. Curvature statistics

We analyzed data produced in a Direct Numerical Simulation of homogeneous and isotropic turbulence in a cubic lattice of 1024^3 grid points [17], corresponding to $\mathcal{R}e_{\lambda} = 284$, seeded with about two millions Lagrangian particles, evolving according to the dynamics

$$\frac{d\mathbf{x}(t)}{dt} = \mathbf{u}(\mathbf{x}(t), t), \quad (3)$$

where $\mathbf{u}(\mathbf{x}, t)$, the fluid velocity field, is a solution of the incompressible Navier–Stokes equations

$$\partial_t \mathbf{u} + (\mathbf{u} \cdot \nabla) \mathbf{u} = -\nabla P + \nu \Delta \mathbf{u} + \mathbf{f} \quad (4)$$

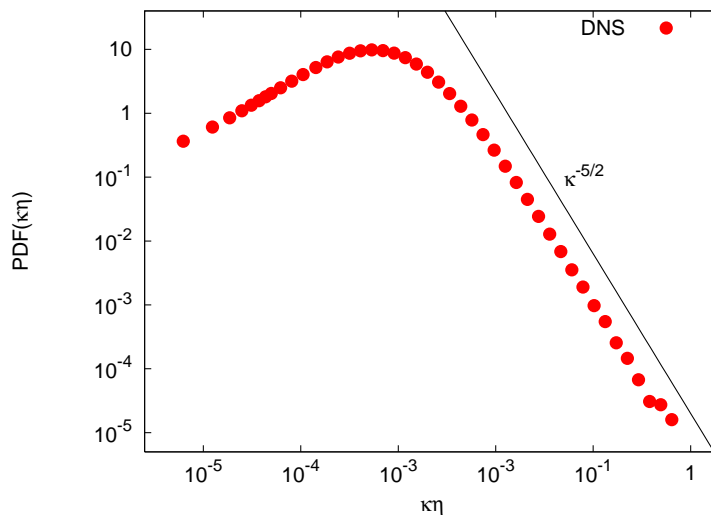


Figure 1. Log–log plot of the curvature PDF, normalized with the dissipative scale η . The solid line represents the $\kappa^{-5/2}$ scaling of the PDF for high curvature values. Data, here and hereafter, come from a high resolution DNS at 1024^3 collocation points, see text for details.

$$\nabla \cdot \mathbf{u} = 0$$

which have been integrated on a triply periodic cubic box by means of a fully dealiased pseudospectral code (energy was injected at an average rate ε by keeping the total energy constant in each of the first two wavenumber shells [21]). The equations (3) have been integrated linearly interpolating the values of the fluid velocity at the lattice sites. Let us stress that the acceleration field we can measure is continuous (and differentiable inside lattice mesh) because it is reconstructed from the local values of pressure gradients, laplacian of velocity and the external forcing along the trajectories. In such a way we can calculate \mathbf{a} directly from the rhs of (4), without performing any differentiation of the particle velocity, thus minimizing noise effects, which are unavoidably present in experiments and, in general, in numerical simulations as well.

2.1. Instantaneous and “time-filtered” curvature

In figure (1) we show the PDF of the instantaneous curvature $\mathcal{P}(\kappa)$. It is possible to notice the same power-law tail $\mathcal{P}(\kappa) \sim \kappa^{-5/2}$, for large curvatures, observed in the numerical simulations by Braun *et al.* [14] and in the experiments by Xu *et al.* [23]. In the latter work it is argued that such a behaviour can be explained considering that the very high curvature events are linked to large scale flow reversals where the particle inverts its motion and its velocity goes to zero, $u^2 \sim 0$. Therefore, the PDF scaling for large curvatures is mainly determined by the Gaussian statistics of the velocity and, in this context, it can be reproduced analytically by simple arguments [23].

In order to avoid contamination from large scale motion, in [23] it was suggested to enhance the contribution of vortex filaments by studying the statistics of the curvature averaged over some time intervals Δ [22]. The *rationale* at the basis of this operation consists in the observation that, while the “trapping” events of particles into the filaments are characterized by a certain degree of temporal persistency (due to the already stated spatio-temporal coherence of such structures), the flow reversals with very low velocity show very little autocorrelation times. Indeed, as also remarked in [23], the larger is the curvature the lesser is the autocorrelation

$\log(\kappa^*)$	τ_{corr}
1.5	$3.8\tau_\eta$
2.5	$1.56\tau_\eta$
3.5	$0.12\tau_\eta$

Table 1. Conditional autocorrelation times and corresponding conditioning thresholds. The autocorrelation times have been extracted from the conditional autocorrelation function of the logarithm of curvature, defined as

$$\mathcal{C}(\tau) = \frac{\langle \log(\kappa(t+\tau)) \log(\kappa(t)) | \log(\kappa(t)) > \log(\kappa^*) \rangle - \langle \log(\kappa(t)) | \log(\kappa(t)) > \log(\kappa^*) \rangle^2}{\langle \log(\kappa(t))^2 | \log(\kappa(t)) > \log(\kappa^*) \rangle - \langle \log(\kappa(t)) | \log(\kappa(t)) > \log(\kappa^*) \rangle^2} \sim e^{-\tau/\tau_{corr}}.$$

At increasing the threshold (including in the computation only higher and higher curvature values) the autocorrelation decreases significantly.

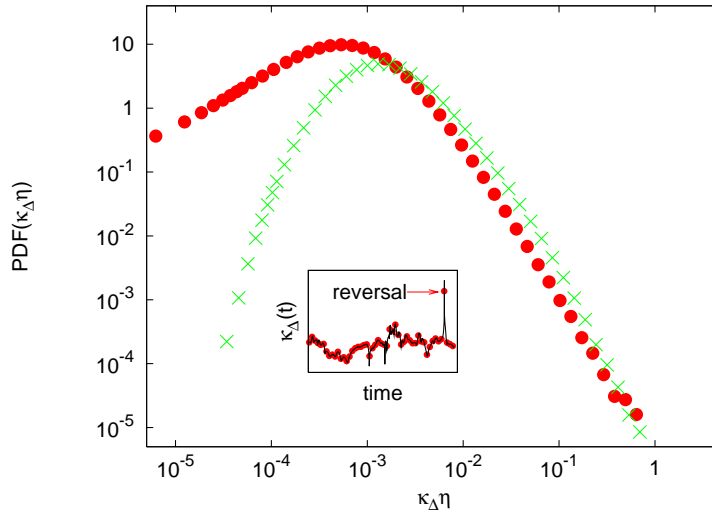


Figure 2. Log-log plot of PDFs of instantaneous (\bullet) and time averaged (\times) curvature (over a window $\Delta = 10\tau_\eta$). It must be noticed that only the tail at low κ values has been effectively damped down by the filtering. *Inset*: Time series of instantaneous (solid line) and time-filtered (\bullet) curvature relative to a trajectory in the high κ tail of $\mathcal{P}(\kappa_{\Delta=10\tau_\eta})$: the arrow highlights the strong flow reversal event which is only very weakly damped by time averaging.

time (in table 1 we report such times extracted from the autocorrelation function of curvature, conditioned on its magnitude, together with the corresponding conditioning threshold). We have, thus, measured the PDFs of the time-filtered curvature:

$$\kappa_\Delta(t) \stackrel{def}{=} \frac{1}{\Delta} \int_{t-\Delta/2}^{t+\Delta/2} \kappa(t') dt' \quad (5)$$

for $\Delta = \tau_\eta, 5\tau_\eta, 10\tau_\eta$, where τ_η is the Kolmogorov time scale. However, even for the greatest time “window” ($10\tau_\eta$), we do not obtain the desired result. In fact, as it is evident from figure (2) where we report the PDFs of instantaneous and time-filtered (with $\Delta = 10\tau_\eta$) curvature, time-filtering is effective mostly at small κ , where the PDF exhibits an important lowering of the tail. The explanation why filtering is not effective at high κ values can be understood with the help of a single example. In the inset of figure (2) we analyse the effect of filtering around a very intense event in our statistics. We superimpose the temporal signal of the curvature together with the filtered one for a trajectory selected at random in the $\mathcal{P}(\kappa_{\Delta=10\tau_\eta})$ tail: at the instant of time at which the event of flow reversal occurs (indicated with an arrow) the curvature becomes so large that it is weakly damped

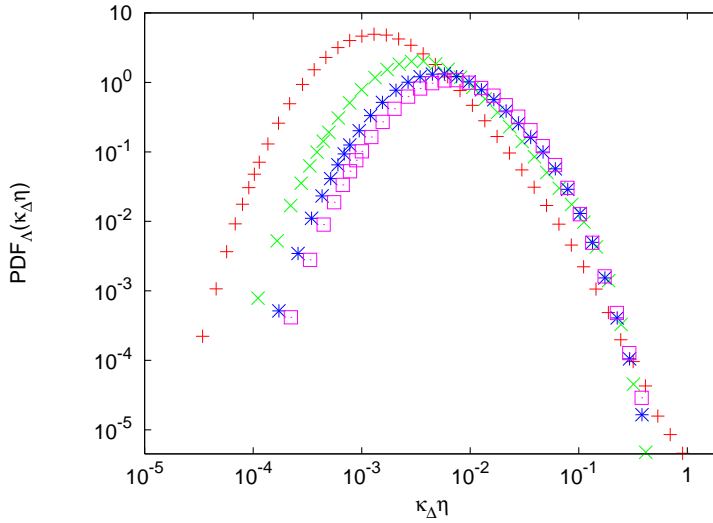


Figure 3. Log-log plot of conditional PDFs (of the time-averaged curvature), computed including only those events for which $u^2 > \Lambda$, for $\Lambda = 0.02u_{rms}^2$ (\times), $0.1u_{rms}^2$ ($*$) and $0.2u_{rms}^2$ (\square), respectively. The introduction of the cutoff induces a change in the slope of the far right tail (we also plot the unconditioned PDF (+) for comparison), reaching an asymptotic shape for the right tail insensitive to the increasing of Λ .

even averaging over the longest time interval we used.

2.2. Vortices identification and analytical results

In order to really focus only on those high-curvature events given by large values of the numerator in (1) we propose to introduce also a *cutoff* (Λ) on the values of the velocity, i.e. we included in the computation of the filtered PDF only those events for which

$$u^2 > \Lambda. \tag{6}$$

We have tried various values Λ , see fig. (3), and observed that there is a tendency toward a PDF shape with a right tail insensitive to the increasing of the cutoff; keeping this in mind we will fix in what follows $\Lambda = 0.02u_{rms}^2$. In this way, we define a *conditional* PDF:

$$\mathcal{P}_\Lambda(\kappa_\Delta) \stackrel{def}{=} \mathcal{P}(\kappa_\Delta | u^2 > \Lambda). \tag{7}$$

As one can observe from figure (4), the application of this constraint results in a dramatic change in the shape of the PDF for high curvature values; in particular, the change of slope of $\mathcal{P}_\Lambda(\kappa_{(\Delta=10\tau_\eta)})$ appears around the value

$$\tilde{\kappa}\eta \equiv \kappa_{(\Delta=10\tau_\eta)}\eta \approx 0.1 \tag{8}$$

where η is the Kolmogorov length. This new shape for the conditional PDF of the time-filtered curvature is compatible (once the two axes are rescaled accordingly) with the PDF of the time-filtered logarithm of the curvature (which was studied in [23]): the reason of the convergence of the two procedures may be due to the fact that, by taking the logarithm of κ , the two terms, the one coming from a_\perp and the other coming from u^2 , contribute now linearly to the curvature, as $\log \kappa = \log(a_\perp) - \log(u^2)$; hence when one performs the time average (which is a

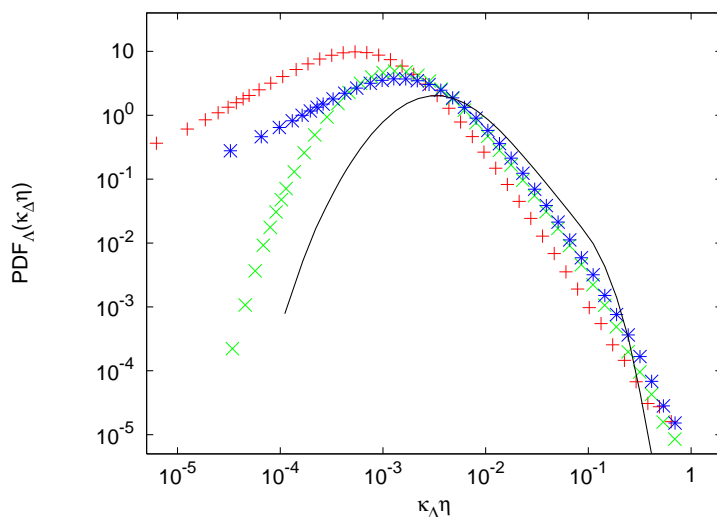


Figure 4. Log-log plot of the PDFs of instantaneous curvature without (+) and with (*) the cutoff on velocity values, and of the PDFs of time-filtered curvature without (x) and with (solid line) the cutoff. It is important to notice that the change of the PDF slope for large curvatures is due to the combination of the two operations (averaging in time and constraining the velocity magnitude).

linear operation) the events at low u^2 values, characterized by short autocorrelation times, are selectively suppressed, similarly to what happens with the introduction of the cutoff. It seems then reasonable to infer that such change of the slope must be attributed to the presence of vortical structures, thus being connected to small scales turbulent properties. Indeed, because of the constraint imposed on u^2 , the highest curvature values are now due to large and temporally persistent accelerations (or, more correctly, to centripetal accelerations). If this is true, the large tail behaviour should be captured by the same multifractal arguments that have been proved successful for describing unconditional acceleration statistics [24], which is highly intermittent [6, 8, 24]. We can write for the curvature PDF (denoted, from now on, with $\mathcal{P}(\kappa)$, for the sake of simplicity) the following expression

$$\mathcal{P}(\kappa) = \int \int \mathcal{P}_{joint}(a, u^2) \delta\left(\kappa - \frac{a}{u^2}\right) \Theta(u^2 - \Lambda) da du, \quad (9)$$

where $\mathcal{P}_{joint}(a, u^2)$ is the joint PDF of a and u^2 , and the Heaviside Θ function has been included to take into account the cutoff on the velocities. Note that we use a for a_{\perp} , neglecting geometrical constraints. Following the multifractal description presented in [24] we may estimate the joint PDF from the relation

$$\mathcal{P}_{joint}(a, u^2) = \delta(a - a(h, u)) \mathcal{P}(u^2); \quad a(h, u) \sim \nu^{\frac{2h-1}{1+h}} u^{\frac{3}{1+h}} L_0^{-\frac{3h}{1+h}} \quad (10)$$

where ν is the viscosity, L_0 is the integral scale (we will keep $L_0 \sim 1$ in the following) and h the scaling exponent characterising the local velocity fluctuation. Let us stress that in the expression of $a(h, u)$ a possible over-all stochastic prefactor, Reynolds independent, can be included, in order to change the degree of correlation between the acceleration and the local velocity field. Such a prefactor would change a bit the joint PDF, but not the global shape of the result. At the Kolmogorov scale, the probability to have an exponent h is given by [24]:

$$\mathcal{P}(h) \sim \left(\frac{\tau_{\eta}}{T_L}\right)^{\frac{3-D(h)}{1-h}} \quad (11)$$

where T_L is the Lagrangian integral time scale and $D(h)$ is the fractal dimension of the set characterised by the exponent h . Using for the probability density of u^2 a third order χ^2 distribution:

$$\mathcal{P}(u^2) \propto u^2 e^{-u^2/2} \quad (12)$$

we obtain:

$$\mathcal{P}(\kappa) \sim \int da \int du \int dh \left(\frac{\nu}{u}\right)^{\frac{3-D(h)}{1+h}} u^2 e^{-\frac{u^2}{2}} \delta\left(a - \nu^{\frac{2h-1}{1+h}} u^{\frac{3}{1+h}}\right) \delta\left(\kappa - \frac{a}{u^2}\right) \Theta(u^2 - \Lambda). \quad (13)$$

Integration over a and u yields the final expression

$$\mathcal{P}(\kappa) \sim \int_{h_{min}}^{h_{max}} \left(\frac{1+h}{1-2h}\right) \nu^3 \kappa^{\frac{5h-1+D(h)}{1-2h}} \exp\left(-\frac{\nu^2 \kappa^{\frac{2(1+h)}{1-2h}}}{2}\right) dh \quad (14)$$

valid for $\kappa \gtrsim 2.0\sigma_\kappa$ (correspondingly $\kappa\eta \gtrsim 0.03$).¹ Working out the integral with $h \in [0.16, 0.38]$ (for integrability reasons exposed in [24]) and using for $D(h)$ the empirical form proposed by She and Lévéque [25] (which was also shown to fit very well experimental data [26], at least in the range of singularity exponents h that we are spanning):

$$D(h) = 1 + p(h) \left(h - \frac{1}{9}\right) + 2 \left(\frac{2}{3}\right)^{\frac{p(h)}{3}} \quad (15)$$

(where $p(h) = (3/\ln(2/3)) \ln[(9h-1)/6\ln(3/2)]$), we have the result shown in figure (5), in excellent agreement with the measured PDF for large curvatures. More in detail, it is worth remarking that the two curves are almost coincident for values of curvature larger than the “critical” value $\tilde{\kappa}$. Let us notice that the good agreement between data and the multifractal formalism only after the introduction of a cutoff in the single point velocity is not an accident. We must expect that phenomenological models based on the energy cascade mechanism work well only for those events that are not dominated by smooth quasi-laminar fluctuations, as it would be the case for the whole curvature statistics without cutoff.

3. Joint statistics of curvature and torsion

Torsion measurements are very difficult in experiments [23] and available only at very low Reynolds numbers in previous numerical works [14]. The difficulty is due to the fact that they involve the time derivative of the acceleration. In our numerical data-base acceleration is differentiable inside mesh grids and continuous everywhere: we could therefore measure torsion with a good signal to noise ratio.

It is natural to suppose that the emergence of coherent structures with peculiar geometries induces somehow a correlation between curvature and torsion of trajectories, as they contain informations on such structures. We studied, then, the joint statistics of the two quantities. We calculated the *residual value* [22] of the

¹This domain limitation arises from the calculation done with the Θ function.

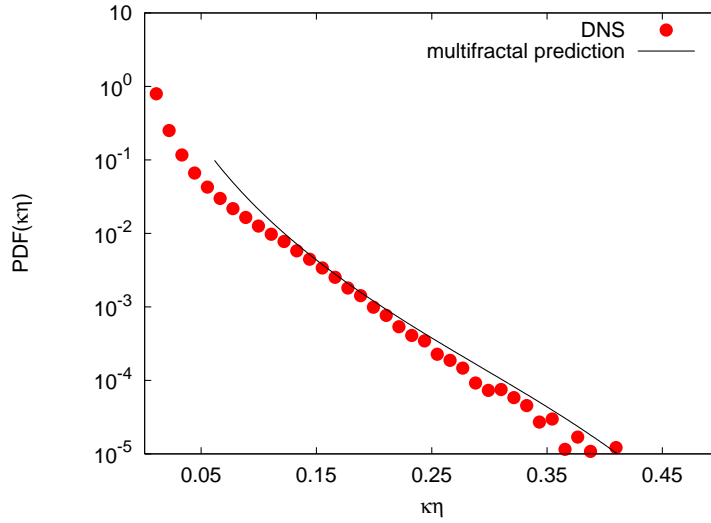


Figure 5. Log–lin plot of the PDF with cutoff on u^2 of the time filtered curvature ($\Delta = 10\tau_\eta$) and the corresponding multifractal prediction.

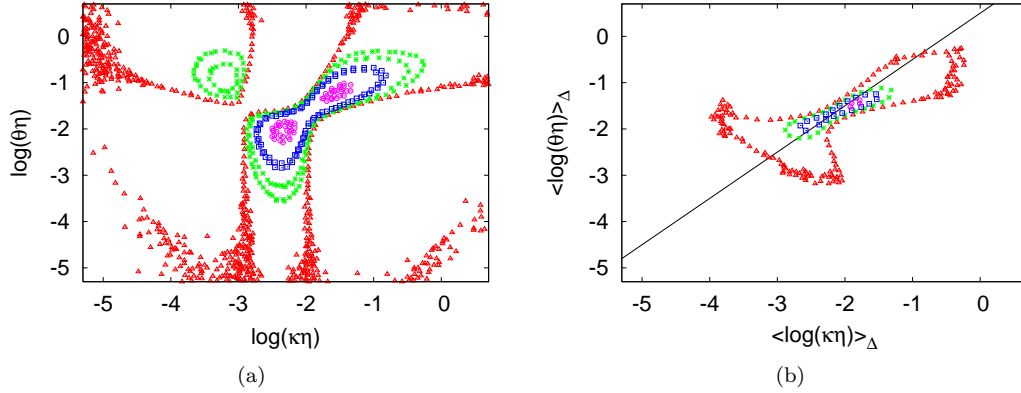


Figure 6. *Residuals* of the logarithms of curvature and torsion, instantaneous (a) and time-averaged (b) over a time window $\Delta = 10\tau_\eta$, plotted as a 2D map with isocontours (only $\mathcal{R} > 0$ is shown). Correlation is lesser on exterior contours. In the right panel we also plot a straight line parallel to the plane bisector $\log(\theta) = \log(\kappa)$.

logarithms of κ and θ , that is the quantity

$$\mathcal{R}(\langle \log(\kappa) \rangle_\Delta, \langle \log(\theta) \rangle_\Delta) \stackrel{\text{def}}{=} \mathcal{P}_{\text{joint}}(\langle \log(\kappa) \rangle_\Delta, \langle \log(\theta) \rangle_\Delta) - \mathcal{P}(\langle \log(\kappa) \rangle_\Delta) \mathcal{P}(\langle \log(\theta) \rangle_\Delta) \quad (16)$$

which quantifies the degree of correlation existing between the two variables. In figure (6) we plot $\mathcal{R}(\log(\kappa), \log(\theta))$ and $\mathcal{R}(\langle \log(\kappa) \rangle_\Delta, \langle \log(\theta) \rangle_\Delta)$, with $\Delta = 10\tau_\eta$, projected onto the $\log(\theta)$ vs $\log(\kappa)$ plane (isocontours are drawn for positive correlation $\mathcal{R} > 0$). In figure (7) we also show the original joint PDF $\mathcal{P}_{\text{joint}}(\langle \log(\kappa) \rangle_\Delta, \langle \log(\theta) \rangle_\Delta)$ for both the instantaneous and time-filtered quantities. The most relevant feature to be stressed is that the effect of time filtering is to accumulate the isocontours to intensify the correlation along the straight lines $\log(\theta) = \log(\kappa) + c$ (parallel to the plane bisector). This equation is exactly what one obtains by taking the logarithm of

$$\theta = \frac{\lambda}{R} \kappa \quad (17)$$

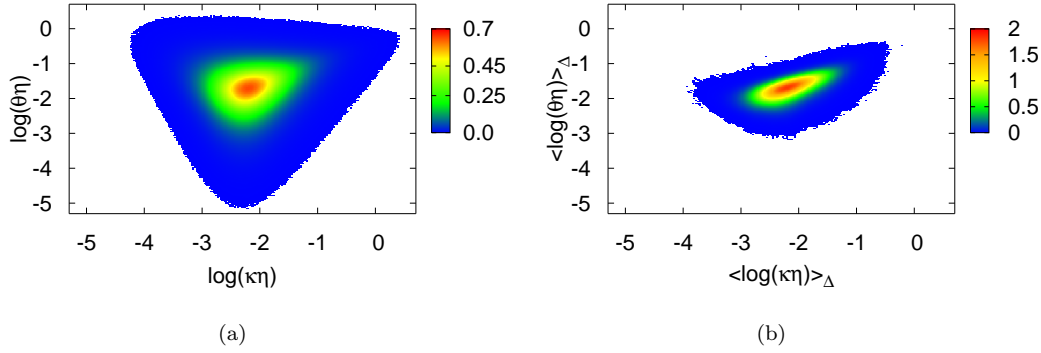


Figure 7. Joint probability distribution functions of the logarithms of curvature and torsion, instantaneous (a) and time-averaged (b) over a time window $\Delta = 10\tau_\eta$.

which is the relation linking torsion and curvature for a “perfect” cylindrical helix (λ being its reduced step and R the cylinder radius), that is the prototype of spatial curve that we imagine when thinking of a vortex tube. From the value of the intercept we can then also estimate the ratio between the step and the radius of the “mean” helix to be $\lambda/r \sim 3$. These two geometrical parameters are related to the inverse curvature (i.e. the radius of curvature) via

$$R = \frac{1}{\kappa} = \frac{r^2 + \lambda^2}{r}; \quad (18)$$

furthermore from the critical value at which the change of slope of the curvature PDF occurs (discussed in the previous section), we get for the radius of curvature $R \sim 10\eta$. Hence, substituting the measured ratio λ/r into (18), we obtain, as an estimate for the radius of the helix,

$$r \sim \eta. \quad (19)$$

These observations strengthen furthermore the conjecture that when filtering and avoiding the very low velocity events, the study of the statistics of curvature and torsion provides an insight on the signatures of vortex filaments.

4. Conclusions

We have analyzed data from DNS of Lagrangian tracers, focusing our attention on the statistics of parameters able to characterize the geometry of particle trajectories, namely curvature and torsion. We found that the statistics of instantaneous curvature is mainly dominated by large scale flow reversal events, rather than by small scale structures like vortex tubes as also found in experimental works in [23]. Indeed, the asymptotics of the PDF can be reproduced by simple Gaussian statistics arguments [23]. In order to unravel small-scales turbulence features, we meant to compute the PDF of curvature averaged in time, including only those events for which the squared velocity magnitude u^2 was greater than a certain threshold, so to avoid the reversals (where $u^2 \sim 0$) and to exalt the statistical signature of vortices. This approach successfully resulted in a marked change of slope in the PDF tail at high curvature values, pointing out the possible presence of vortex filaments. The criterion here presented is therefore different from what proposed in other works

[15]. Moreover, we could derive an analytical expression for $\mathcal{P}_\Lambda(\kappa_\Delta)$, in the context of the multifractal formalism, which fits well the far tails, providing an interesting matching between geometry and phenomenology. The analysis of joint statistics of curvature and torsion has been also addressed, confirming our statements on the topology of coherent small scale structures.

Acknowledgements

I gratefully thank Luca Biferale for his precious suggestions and support. I would also like to acknowledge useful and interesting discussions with Federico Toschi and Alessandra Lanotte.

References

- [1] S.B. Pope, *Turbulent Flows*, Cambridge University Press (2000).
- [2] P.K. Yeung, “Lagrangian investigation of turbulence”, *Annu. Rev. Fluid Mech.* **34**, 115 (2002).
- [3] G. Falkovich, A. Fouxon and M. Stepanov, “Acceleration of rain initiation by cloud turbulence”, *Nature* (London) **419**, 151 (2002).
- [4] S. Post and J. Abraham, “Modeling the outcome of drop–drop collisions in diesel sprays”, *Int. J. Multiphase Flow* **28**, 997 (2002).
- [5] B. Sawford, “Turbulent relative dispersion”, *Annu. Rev. Fluid Mech.* **33**, 289 (2001).
- [6] A. La Porta, G. A. Voth, A. M. Crawford, J. Alexander and E. Bodenschatz, “Fluid particle accelerations in fully developed turbulence”, *Nature*, **409**, 1017 (2001).
- [7] A. Arneodo, J. Berg, R. Benzi, L. Biferale, E. Bodenschatz, A. Busse, E. Calzavarini, B. Castaing, M. Cencini, L. Chevillard, R. Fisher, R. Grauer, H. Homann, D. Lamb, A.S. Lanotte, E. L ev eque, B. L uthi, J. Mann, N. Mordant, W.–C. Muller, S. Ott, N.T. Ouellette, J.–F. Pinton, S.B. Pope, S.G. Roux, F. Toschi, H. Xu and P.K. Yeung, “Universal intermittent properties of particle trajectories in highly turbulent flows”, *Phys. Rev. Lett.* **100**, 254504 (2008).
- [8] N. Mordant, P. Metz, O. Michel and J.–F. Pinton, “Measurement of Lagrangian velocity in fully developed turbulence”, *Phys. Rev. Lett.* **87**, 214501 (2001).
- [9] S. Ott and J. Mann, “An experimental investigation of the relative diffusion of particle pairs in three–dimensional turbulent flow”, *J. Fluid Mech.* **422**, 207 (2000).
- [10] B. L uthi, A. Tsinober and W. Kinzelbach, “Lagrangian measurement of vorticity dynamics in turbulent flow”, *J. Fluid Mech.* **528**, 87 (2005).
- [11] F. Toschi and E. Bodenschatz, “Lagrangian properties of particles in turbulence”, *Annu. Rev. Fluid Mech.* (to appear in 2009).
- [12] H.K. Moffatt and A. Tsinober, “Helicity in laminar and turbulent flow”, *Annu. Rev. Fluid Mech.* **24**, 281–312 (1992).
- [13] G. Sposito, “Topological groundwater hydrodynamics”, *Adv. in Wat. Res* **24**, 793–801 (2001).
- [14] W. Braun, F. De Lillo and B. Eckhardt, “Geometry of particle paths in turbulent flows”, *Journ. Turbulence* **7**, 62 (2006).
- [15] F. Moisy and J. Jim enez, “Geometry and clustering of intense structures in isotropic turbulence”, *J. Fluid Mech.* **513**, 111–133 (2004).
- [16] L. Biferale, G. Boffetta, A. Celani, A. Lanotte and F. Toschi, “Lagrangian statistics in fully developed turbulence”, *Journ. Turbulence* **7**, 6 (2006).
- [17] L. Biferale, G. Boffetta, A. Celani, A. Lanotte and F. Toschi, “Particle trapping in three dimensional fully developed turbulence”, *Phys. Fluids* **17**, 021701 (2005).
- [18] J.K. Eaton and J.R. Fessler, “Preferential concentrations of particles by turbulence”, *Int. J. Multiphase Flow* **20**, 169 (1994).
- [19] J. Bec, L. Biferale, M. Cencini, A.S. Lanotte and F. Toschi, “Effects of vortex filaments on the velocity of tracers and heavy particles in turbulence”, *Phys. Fluids* **18**, 081702 (2006).
- [20] J. Bec, L. Biferale, G. Boffetta, A. Celani, M. Cencini, A. Lanotte, S. Musacchio and F. Toschi, “Acceleration statistics of heavy particles in turbulence”, *J. Fluid Mech.* **550**, 349 (2006).
- [21] S. Chen, G. D. Doolen, R. H. Kraichnan and Z–S She, “On statistical correlations between velocity increments and locally averaged dissipation in homogeneous turbulence”, *Phys. Fluids A* **5**, 458 (1993).
- [22] L. Biferale and F. Toschi, “Joint statistics of acceleration and vorticity in fully developed turbulence”, *Journ. Turbulence* **6**, 1 (2006).
- [23] H. Xu, N.T. Ouellette and E. Bodenschatz, “Curvature of Lagrangian trajectories in turbulence”, *Phys. Rev. Lett.* **98**, 050201 (2007).
- [24] L. Biferale, G. Boffetta, A. Celani, B.J. Devenish, A. Lanotte and F. Toschi, “Multifractal statistics of Lagrangian velocity and acceleration in turbulence”, *Phys. Rev. Lett.* **93**, 064502 (2004).
- [25] Z–S. She and E. L ev eque, “Universal scaling laws in fully developed turbulence”, *Phys. Rev. Lett.* **72**, 336 (1994).
- [26] H. Xu, N.T. Ouellette and E. Bodenschatz, “Multifractal dimension of Lagrangian turbulence”, *Phys. Rev. Lett.* **96**, 114503 (2006).